APPLIED PHYSICS LETTERS 104, 041117 (2014)

Hydrogen peroxide detection with quartz-enhanced photoacoustic spectroscopy using a distributed-feedback quantum cascade laser

Wei Ren,[1,a)] Wenzhe Jiang,[1] Nancy P. Sanchez,[2] Pietro Patimisco,[1,3] Vincenzo Spagnolo,[3] Chung-en Zah,[4] Feng Xie,[4] Lawrence C. Hughes,[4] Robert J. Griffin,[2] and Frank K. Tittel[1]
[1]*Department of Electrical and Computer Engineering, Rice University, 6100 Main Street, Houston, Texas 77005, USA*
[2]*Department of Civil and Environmental Engineering, Rice University, 6100 Main Street, Houston, Texas 77005, USA*
[3]*Dipartimento Interateneo di Fisica, Università e Politecnico di Bari, Via Amendola 173, Bari 70126, Italy*
[4]*Corning Incorporated, Corning, New York 14831, USA*

(Received 10 December 2013; accepted 19 January 2014; published online 31 January 2014)

A quartz-enhanced photoacoustic spectroscopy sensor system was developed for the sensitive detection of hydrogen peroxide (H_2O_2) using its absorption transitions in the v_6 fundamental band at ~7.73 μm. The recent availability of distributed-feedback quantum cascade lasers provides convenient access to a strong H_2O_2 absorption line located at 1295.55 cm^{-1}. Sensor calibration was performed by means of a water bubbler that generated titrated average H_2O_2 vapor concentrations. A minimum detection limit of 12 parts per billion (ppb) corresponding to a normalized noise equivalent absorption coefficient of 4.6×10^{-9} $cm^{-1}W/Hz^{1/2}$ was achieved with an averaging time of 100 s. © *2014 AIP Publishing LLC*. [http://dx.doi.org/10.1063/1.4863955]

Hydrogen peroxide (H_2O_2) has been identified as an important atmospheric species, playing a major role in the oxidative capacity of the atmosphere and in the balance of HO_x radicals (OH and HO_2).[1–3] H_2O_2 also constitutes a critical oxidant specie in the in-cloud oxidation of S(IV) to S(VI), which is associated with phenomena such as acid rain formation.[1] In addition to its environmental relevance, H_2O_2 vapor also can be used as the active agent in decontamination and sterilization systems intended for hospital rooms as well as medical and industrial equipment.[4–6] Furthermore, levels of H_2O_2 in breath are used as a marker of oxidative stress associated with pulmonary conditions such as lung cancer and chronic obstructive pulmonary disease.[7,8]

A sensitive and reliable H_2O_2 detection system is thus useful for atmospheric chemistry research, industrial process monitoring and control, and medical diagnostics. The determination of gas-phase H_2O_2 is typically performed using wet chemistry methods including colorimetry after formation of a Ti-H_2O_2 complex, luminol-based chemiluminescence, and peroxidase-catalyzed reaction for subsequent quantification by fluorescence spectroscopy.[1,9] However, the transfer from the gas-phase H_2O_2 to the liquid phase for subsequent wet-chemistry based analysis can lead to sampling artifacts and interferences by other constituents in the atmosphere.[9] Therefore, the direct measurement of gas-phase H_2O_2 offers inherent advantages.

Several optical sensing techniques have been employed for H_2O_2 detection in the gas-phase. H_2O_2 detection by kilometer optical path length Fourier transform infrared spectroscopy was reported, with estimated detection limits between 40 and 100 ppb.[10] Tunable diode laser absorption spectroscopy, combined with a multipass White cell and wavelength-modulation approach, was applied for the determination of H_2O_2 in ambient air with a ppb-level detection limit for measurement times of several minutes.[11] A compact H_2O_2 sensor platform consisting of an astigmatic multipass cell and a quantum cascade laser as the light source has been demonstrated, showing a detection limit of 15 ppb, while employing several thousands of co-added spectra, leading to an acquisition time of longer than 1 h.[12] H_2O_2 detection using cavity-enhanced optical frequency comb spectroscopy at ~3.76 μm was reported to achieve a detection limit of 130 ppb in the presence of 2.8% water.[13] Recently, a sensitive measurement of H_2O_2 was reported with a distributed-feedback quantum cascade laser (DFB-QCL) operating at 1283.326 cm^{-1} to achieve a concentration noise level of 110 parts per trillion (ppt) at 1 s averaging time.[14] In this technique, an astigmatic Herriott absorption cell with a volume of 2 l was utilized to obtain a total path length of 250 m (554 passes).

One of the most robust and sensitive trace-gas optical detection techniques is quartz-enhanced photoacoustic spectroscopy (QEPAS).[15] QEPAS allows performance of sensitive measurements in a very small (few mm^3) gas sample, which is suitable for applications requiring a compact, lightweight, and low cost sensor architecture.[16–22] In this technique, a quartz tuning fork (QTF, intended for use as a frequency standard in electronic clocks) is applied as a sharply resonant acoustic transducer to detect weak acoustic waves, in contrast to a broadband electric microphone used in conventional photoacoustic spectroscopy (CPAS).

In this Letter, a QEPAS system developed for sensitive gas-phase H_2O_2 detection using a continuous wave (cw) thermoelectrically cooled (TEC) DFB-QCL at ~7.73 μm is reported. This sensor provided unambiguous identification of the H_2O_2 absorption feature with no interference from other atmospheric gases. Calibration techniques also have been described and conducted to demonstrate the sampling procedures. The response of the QEPAS signals is linear with the H_2O_2 mixing ratio and a detection limit of 12 ppb is estimated for a 100 s averaging time.

a)Electronic mail: wr5@rice.edu

The experimental setup is schematically depicted in Fig. 1. A cw, DFB-QCL (Corning Incorporated, New York, USA) operating at ~7.73 μm was used as a QEPAS laser excitation source. The laser current and temperature were controlled by a commercial current source (ILX Lightwave, LDX 3220) and a temperature controller (Wavelength Electronics, MPT10000), respectively. After tuning the laser injection current to the target wavelength near 7.73 μm (25 °C, 260 mA), the laser output power was measured to be ~80 mW and a maximum output power of 120 mW. Two plano-convex ZnSe lenses, L_1 (focal length f = 45 mm) and L_2 (f = 25 mm), and a pinhole spatial filter with a diameter of 300 μm were used to improve the QCL beam quality. The QCL beam was directed through two micro-resonator (mR) tubes via L_2 and focused between the two prongs of the QTF, located inside an absorption detection module (ADM). An optical power meter (Ophir, model 3A-SH) was used to monitor the transmitted optical power from the QCL passing through the ADM for alignment verification. The entire optical/electric system can be mounted on a platform with dimensions of 35 cm × 30 cm × 25 cm.

H_2O_2 vapor was prepared and controlled by flowing a carrier gas (pure N_2 or air) over a 30% weight-to-weight aqueous H_2O_2 solution (EMD Millipore, USA). In order to obtain gas samples with different concentrations, the generated H_2O_2 vapor mixtures were mixed with another stream of pure N_2 and both flow rates were controlled by mass flow controllers (MKS Instruments Inc.), as illustrated in Fig. 1. The combined flow then entered the ADM for QEPAS measurements after flowing through a 2-m long Teflon@ tube for thorough mixing.

Gas sensors are typically calibrated with a calibrated commercial gas cylinder, however, H_2O_2 is not available commercially in a cylinder because it is unstable and decomposes naturally to water and oxygen. However, the test gas mixture containing H_2O_2 vapor can be bubbled through a water bubbler that captures the H_2O_2 molecules, enabling the time-averaged H_2O_2 concentration to be determined subsequently.[23] In this work, the gas flow from the ADM outlet was bubbled through a known volume (100 ml) of deionized water for 1-2 h, with the final concentration to be determined by titration with potassium permanganate ($KMnO_4$). The efficiency of H_2O_2 collection was estimated to be >99%, considering the high solubility of H_2O_2 in water. A 5 ml aliquot obtained from the collected 100 ml H_2O_2 solution was titrated against a known concentration of $KMnO_4$ according to the following reaction:

$$5H_2O_2 + 3H_2SO_4 + 2KMnO_4 \rightarrow 5O_2 + K_2SO_4 + 8H_2O + 2MnSO_4, \quad \text{(R1)}$$

from which the number of moles of H_2O_2 (n_{H2O2}) in the solution is determined. Hence, the average H_2O_2 vapor mixing ratio ($\bar{c}_{H2O2}$) during the entire process is obtained *via* $\bar{c}_{H2O2} = n_{H2O2}/n_{total}$. The total number of moles of mixtures n_{total} can be calculated from the known sample collection time and total gas flow rate. The connection between the ADM and water bubbler was kept to minimum length to reduce the possible breakdown of H_2O_2, so that the gas mixtures inside the ADM and into the water bubbler have the same H_2O_2 concentration. Additionally, a needle valve combined with a vacuum pump at the outlet of the water bubbler was used to control and maintain a constant gas pressure inside the ADM.

Wavelength modulation spectroscopy (WMS) with second harmonic (2f) detection was utilized for sensitive H_2O_2 QEPAS measurements. In WMS, a voltage ramp is applied to the current driver to scan across the absorption feature of the target gas while a sinusoidal dither is applied at half of the QTF resonant frequency (f = $f_0/2$~16.3 kHz). The piezoelectric signal generated by the QTF was detected by a custom-designed transimpedance amplifier with a 10 MΩ feedback resistor. This amplified signal was subsequently demodulated at the QTF resonant frequency (f_0) to obtain its second harmonic component (QEPAS 2f signal) using a commercial control electronics unit (CEU). The CEU also has the function of measuring the QTF parameters (i.e., quality factor $Q \sim 14000$, dynamic resistance R ~ 94 kΩ, and resonant frequency $f_0 \sim 32.7$ kHz measured at the pressure of 80 torr) and modulating the laser injection current.

The H_2O_2 absorption lines in the v_6 fundamental ro-vibrational band related to the O-H asymmetric bend mode were used in this study for sensitive H_2O_2 detection.

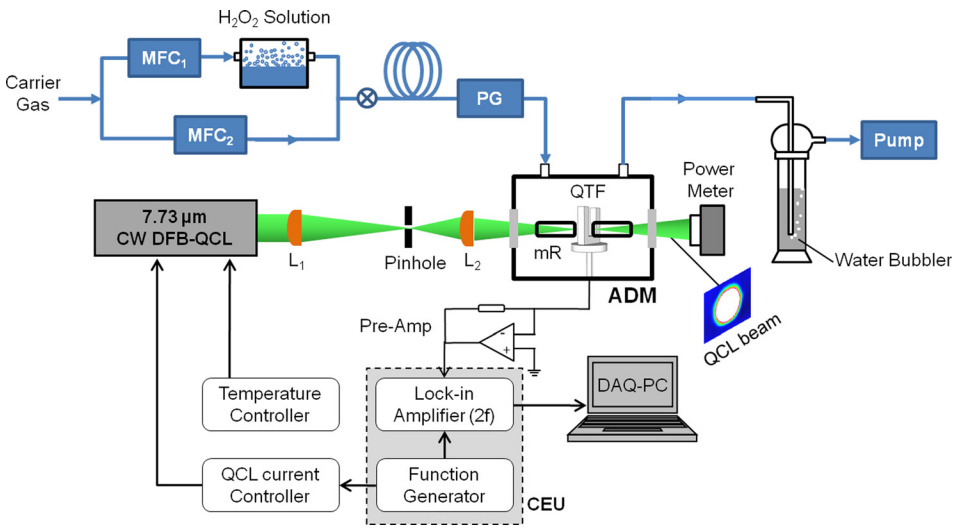

FIG. 1. Schematic of a cw DFB-QCL based QEPAS system for H_2O_2 detection and calibration. ADM, absorption detection module; CEU, control electronics unit; MFC, mass flow controller; PG, pressure gauge; mR, micro-resonator.

Due to the molecular similarity, the H_2O_2 absorption band has relatively strong overlap with that of H_2O. The HITRAN database[24] was used to identify specific QCL frequencies for interference-free H_2O_2 detection. Figure 2 (bottom panel) presents the specific spectral region of interest near 1295 cm^{-1}, which is simulated for 1 ppm H_2O_2/air at 296 K and 15 torr. The QEPAS 2f signal within the same wavelength range (Fig. 2, top panel) also was recorded at 296 K and 15 torr. A relatively low pressure was chosen in order to obtain resolved features in the spectra. The QCL wavelength was calibrated using a Fourier-transform interferometer in the rapid-scan mode with a resolution of 0.125 cm^{-1}. Another two QEPAS 2f spectral scans acquired when pure N_2 and standard air were introduced into the ADM also are plotted in Fig. 2 (top panel) for comparison. Such a comparison of three spectral scans indicates that this wavelength range is free from interference of common air constituents (i.e., H_2O, CO_2, CO, N_2O, and CH_4). Therefore, the H_2O_2 absorption near 1295.55 cm^{-1} was selected in this study for QEPAS sensor development due to its relatively stronger absorption strength.

To maximize the QEPAS 2f signal, the total gas pressure, the wavelength modulation depth and the phase of the demodulated QEPAS 2f signal must be appropriately chosen.[15] A combined $H_2O_2/H_2O/N_2$ gas flow ($MFC_1 = 30$ sccm, $MFC_2 = 170$ sccm, resulting in a titrated H_2O_2 mixing ratio of 14 ppm) was prepared and introduced into the ADM. Figure 3 depicts the pressure-dependent QEPAS 2f amplitude near 1295.55 cm^{-1} at four different modulation depths. It can be seen that the 2f amplitude varies significantly with pressure in the range of 80 torr to 130 torr. The wavelength modulated 2f signal increases when the total gas pressure decreases due to the narrowing effect of the absorption feature. Additionally, the Q-factor of the quartz tuning fork increases at lower pressures, also resulting in higher QEPAS signal, S, as the QEPAS amplitude is proportional to the following parameters:

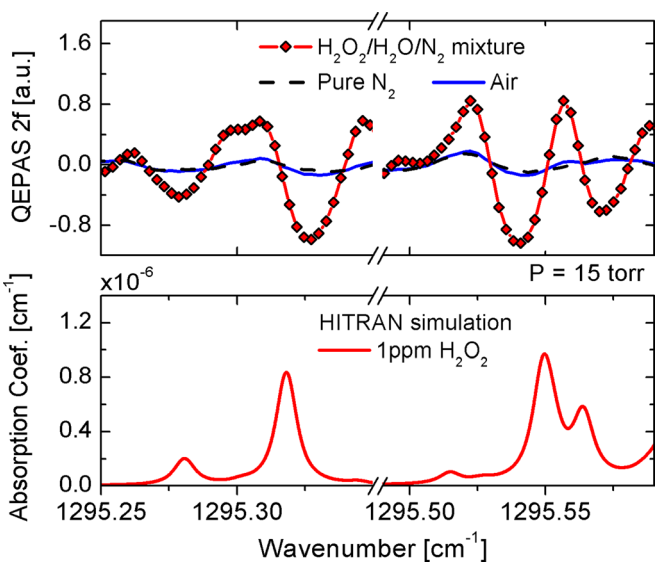

FIG. 2. Comparison of the measured H_2O_2 QEPAS signal (top panel) and the simulated H_2O_2 spectra (bottom panel) at $P = 15$ torr. QEPAS signal was recorded at the specific flow rates of $MFC_1 = 20$ sccm, $MFC_2 = 180$ sccm; simulation was performed using the HITRAN database[24] for 1 ppm H_2O_2 in air.

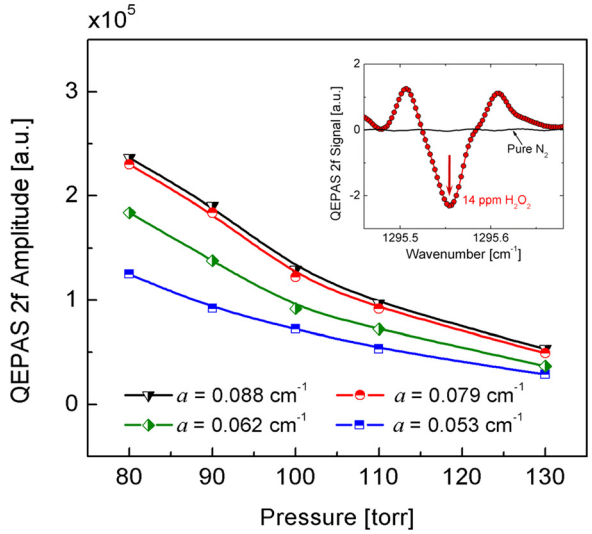

FIG. 3. Measured QEPAS 2f amplitude for a specific $H_2O_2/H_2O/N_2$ mixture ($MFC_1 = 30$ sccm, $MFC_2 = 170$ sccm, resulting in a titrated H_2O_2 mixing ratio of 14 ppm) as a function of the total gas pressure at four different modulation depths. Inset: a representative QEPAS 2f profile using the modulation depth of 0.079 cm^{-1} and pressure of 80 torr.

$$S \propto \frac{\alpha P Q}{f_0}, \tag{1}$$

where α is the absorption coefficient of the target species, P is the optical power, Q and f_0 are the quality factor and the resonant frequency of the QTF, respectively. A reduction of the gas pressure causes the molecular collision rate and thus the V-T (vibration-to-translation) relaxation rate to decrease. Hence, local gas heating cannot follow fast changes of the laser induced molecular vibration excitation. In the investigated gas pressure range, the H_2O_2 QEPAS signal increases with decreasing pressure, demonstrating that the signal enhancement due to higher Q-factors compensates a decrease of both the V-T relaxation rate and the absorption coefficient (see Fig. 3). However, at a certain lower pressure, the QEPAS signal is expected to start decreasing when the pressure dependent absorption coefficient and V-T relaxation rate dominate the contribution to the QEPAS signal.[25,26] In our measurements, it is necessary to operate at a gas pressure of >80 torr, constrained by the water bubbler design used for collecting H_2O_2 molecules (in order to minimize an unstable gas flux). It may be possible that higher QEPAS signals could be achieved if working at lower pressure, thereby enhancing the H_2O_2 detectivity with the current sensor configuration.

Furthermore, higher 2f amplitude can be achieved with a larger modulation depth as shown in Fig. 3. However, the 2f amplitude reaches a quasi-plateau level when the modulation depth is larger than 0.079 cm^{-1}. Therefore, a gas pressure of 80 torr inside the ADM and a modulation depth of 0.079 cm^{-1} were selected for optimum QEPAS based H_2O_2 sensing. A representative QEPAS 2f signal for 14 ppm H_2O_2 is shown in the inset graph of Fig. 3, along with the recorded background signal (pure N_2 passed through the ADM).

The QEPAS sensor calibration was performed by passing the gas flow from the ADM into the water bubbler as illustrated in Fig. 1. The H_2O_2 vapor flow was required to be

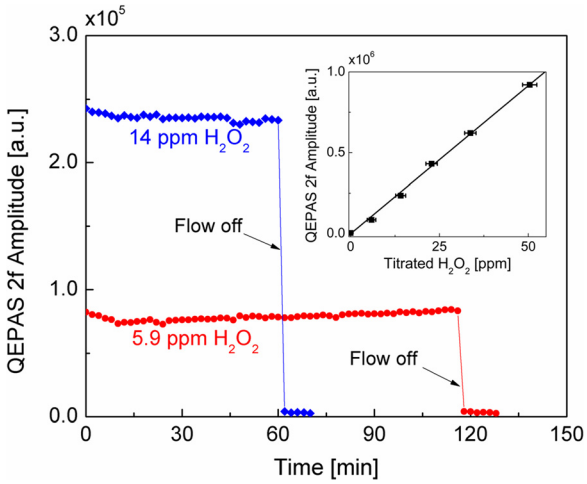

FIG. 4. Measured QEPAS 2f amplitude as a function of time for two H_2O_2 flow streams with different mixing ratios. Inset: the linearity of the QEPAS 2f amplitude to the titrated H_2O_2 vapor.

stable during the bubbling process so that the titrated H_2O_2 concentration can be assigned to the measured QEPAS signal. The stability of H_2O_2 flow was confirmed (within a standard deviation of 5%) by scanning the laser wavelength across the selected H_2O_2 absorption feature and measuring the QEPAS 2f amplitude, as shown in Fig. 4 for two H_2O_2 gas flow streams with different mixing ratios. The averaged QEPAS 2f amplitude as a function of the titrated H_2O_2 concentration (0–55 ppm) is also presented in Fig. 4 (inset graph). The linear fitting gives the R-square value of 0.998, indicating a good linear response of the sensor to monitor H_2O_2 vapor concentrations. For each measurement, the test gas mixture was bubbled into water for 1–2 h to reach a sufficiently high H_2O_2 concentration in the solution for titration. All experiments were performed at 80 torr inside the ADM and with a wavelength modulation depth of 0.079 cm^{-1}.

An Allan deviation analysis was performed to investigate the long-term stability and precision of the H_2O_2 QEPAS sensor. In this case, the center wavelength of the QCL was set to monitor the QEPAS 2f amplitude while pure N_2 was passed through the sensor system. The Allan deviation shown in Fig. 5 reveals that the detection limit can be improved from 75 ppb at 1 s integration time to 12 ppb

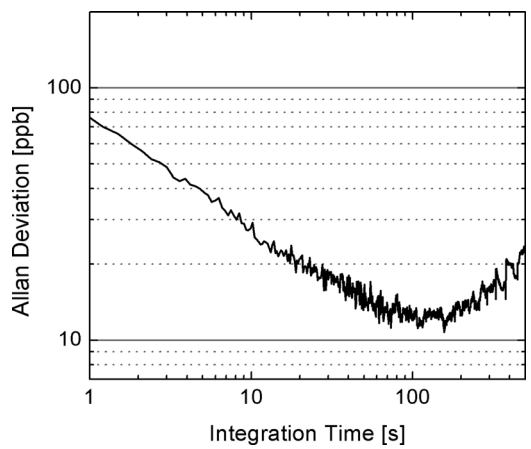

FIG. 5. Allan deviation in ppb of the QEPAS 2f signal as a function of integration time.

corresponding to a normalized noise equivalent absorption (NNEA) coefficient of 4.6×10^{-9} $cm^{-1}W/Hz^{1/2}$ at the integration time of 100 s.

In conclusion, we have demonstrated sensitive QEPAS-based H_2O_2 detection with a fast response time using a cw TEC distributed-feedback quantum cascade laser. A strong absorption line of H_2O_2 at 1295.55 cm^{-1} was identified and used for the interference-free H_2O_2 measurement. Sensor calibration was performed by placing the absorption detection module in series with a water bubbler, and using the generated titrated average vapor concentration. The minimum detection limit for the current QEPAS-based H_2O_2 sensor is estimated to be 75 ppb with a 1 s integration time and can be improved to be 12 ppb at the optimal integration time of 100 s. This sensor can be potentially used for H_2O_2 detection in breath for the diagnosis of acute respiratory distress syndrome.

The Rice University group acknowledges financial support from a National Science Foundation (NSF) ERC MIRTHE award, a NSF-ANR award for international collaboration in chemistry, "Next generation of Compact Infrared Laser based Sensor for Environmental monitoring (NexCILAS)," and the Robert Welch Foundation grant C-0586. P. Patimisco and V. Spagnolo acknowledge financial support from three Italian research projects: PON01_02238, PON02_00675, and PON02_ 00576.

[1]H. Sakugawa, I. R. Kaplan, W. Tsai, and Y. Cohen, Environ. Sci. Technol. **24**, 1452 (1990).
[2]T. Klippel, H. Fischer, H. Bozem, M. G. Lawrence, T. Butler, P. Jöckel, H. Tost, M. Martinez, H. Harder, E. Regelin, R. Sander, C. L. Schiller, A. Stickler, and J. Lelieveld, Atmos. Chem. Phys. **11**, 4391 (2011).
[3]M. Lee, B. G. Heikes, D. J. Jacob, G. Sachse, and B. Anderson, J. Geophys. Res. Atmos. **102**, 1301 (1997).
[4]N. A. Klapes and D. Vesley, Appl. Environ. Microb. **56**, 503 (1990).
[5]B. C. Webb, PDA J. Pharm. Sci. Tech. **55**, 49 (2001).
[6]T. Holmdahl, P. Lanbeck, M. Wullt, and M. H. Walder, Infect. Control Hosp. Epidemiol. **32**, 831 (2011).
[7]H. P. Chan, V. Tran, C. Lewis, and P. S. Thomas, J. Thorac. Oncol. **4**, 172 (2009).
[8]W. MacNee, Proc. Am. Thorac. Soc. **2**, 50 (2005).
[9]M. Lee, B. G. Heikes, and D. W. O'Sullivan, Atmos. Environ. **34**, 3475 (2000).
[10]E. C. Tuazon, A. M. Winer, R. A. Graham, and J. N. Pitts, Adv. Environ. Sci. Technol. **10**, 259 (1980).
[11]F. Slemr, G. W. Harris, D. R. Hastie, G. I. Mackay, and H. I. Schiff, J. Geophys. Res. Atmos. **91**, 5371 (1986).
[12]R. Lindley, E. Normand, M. McCulloch, P. Black, I. Howieson, C. Lewis, and B. Foulger, Proc. SPIE **7119**, 71190K (2008).
[13]A. Foltynowicz, P. Masłowski, A. J. Fleisher, B. J. Bjork, and J. Ye, Appl. Phys. B **110**, 163 (2013).
[14]J. B. McManus, M. S. Zahniser, and D. D. Nelson, Appl. Opt. **50**, A74 (2011).
[15]A. A. Kosterev, Y. A. Bakhirkin, R. F. Curl, and F. K. Tittel, Opt. Lett. **27**, 1902 (2002).
[16]D. Weidmann, A. A. Kosterev, F. K. Tittel, N. Ryan, and D. McDonald, Opt. Lett. **29**, 1837 (2004).
[17]A. A. Kosterev, F. K. Tittel, D. V. Serebryakov, A. L. Malinovsky, and I. V. Morozov, Rev. Sci. Instrum. **76**, 043105 (2005).
[18]S. Gray, A. Liu, F. Xie, and C. Zah, Opt. Express **18**, 23353 (2010).
[19]H. Yi, K. Liu, W. Chen, T. Tan, L. Wang, and X. Gao, Opt. Lett. **36**, 481 (2011).
[20]V. Spagnolo, P. Patimisco, S. Borri, G. Scamarcio, B. E. Bernacki, and J. Kriesel, Opt. Lett. **37**, 4461 (2012).
[21]S. Borri, P. Patimisco, A. Sampaolo, H. E. Beere, D. A. Ritchie, M. S. Vitiello, G. Scamarcio, and V. Spagnolo, Appl. Phys. Lett. **103**, 021105 (2013).

[22]P. Patimisco, G. Scamarcio, F. K. Tittel, and V. Spagnolo, "Quartz-enhanced photoacoustic spectroscopy: A review," Sensors (submitted).
[23]N. St Hill and G. Turner, Anal. Methods **3**, 1901 (2011).
[24]L. S. Rothman, I. E. Gordon, A. Barbe, D. C. Benner, P. F. Bernath, M. Birk, V. Boudon, L. R. Brown, A. Campargue, J.-P. Champion, K. Chance, L. H. Coudert, V. Dana, V. M. Devi, S. Fally, J.-M. Flaud, R. R. Gamache, A. Goldman, D. Jacquemart, I. Kleiner, N. Lacome, W. J. Lafferty, J.-Y. Mandin, S. T. Massie, S. N. Mikhailenko, C. E. Miller, N. Moazzen-Ahmadi, O. V. Naumenko, A. V. Nikitin, J. Orphal, V. I. Perevalov, A. Perrin, A. Predoi-Cross, C. P. Rinsland, M. Rotger, M. Šimečková, M. A. H. Smith, K. Sung, S. A. Tashkun, J. Tennyson, R. A. Toth, A. C. Vandaele, and J. Vander Auwera, J. Quant. Spectrosc. Radiat. Transfer **110**, 533 (2009).
[25]A. A. Kosterev, Y. A. Bakhirkin, F. K. Tittel, S. Mcwhorter, and B. Ashcraft, Appl. Phys. B **92**, 103 (2008).
[26]L. Dong, V. Spagnolo, R. Lewicki, and F. K. Tittel, Opt. Express **19**, 24037 (2011).